The effects of seasonal and diurnal variations in the Earth's magnetic dipole orientation on solar wind–magnetosphere-ionosphere coupling

Ingrid Cnossen,[1] Michael Wiltberger,[1] and Jeremy E. Ouellette[2]

Received 13 April 2012; revised 19 September 2012; accepted 10 October 2012; published 16 November 2012.

[1] The angle μ between the geomagnetic dipole axis and the geocentric solar magnetospheric (GSM) z axis, sometimes called the "dipole tilt," varies as a function of UT and season. Observations have shown that the cross-polar cap potential tends to maximize near the equinoxes, when on average $\mu = 0$, with smaller values observed near the solstices. This is similar to the well-known semiannual variation in geomagnetic activity. We use numerical model simulations to investigate the role of two possible mechanisms that may be responsible for the influence of μ on the magnetosphere-ionosphere system: variations in the coupling efficiency between the solar wind and the magnetosphere and variations in the ionospheric conductance over the polar caps. Under southward interplanetary magnetic field (IMF) conditions, variations in ionospheric conductance at high magnetic latitudes are responsible for 10–30% of the variations in the cross-polar cap potential associated with μ, but variations in solar wind–magnetosphere coupling are more important and responsible for 70–90%. Variations in viscous processes contribute slightly to this, but variations in the reconnection rate with μ are the dominant cause. The variation in the reconnection rate is primarily the result of a variation in the length of the section of the separator line along which relatively strong reconnection occurs. Changes in solar wind–magnetosphere coupling also affect the field-aligned currents, but these are influenced as well by variations in the conductance associated with variations in μ, more so than the cross-polar cap potential. This may be the case for geomagnetic activity too.

Citation: Cnossen, I., M. Wiltberger, and J. E. Ouellette (2012), The effects of seasonal and diurnal variations in the Earth's magnetic dipole orientation on solar wind–magnetosphere-ionosphere coupling, *J. Geophys. Res.*, *117*, A11211, doi:10.1029/2012JA017825.

1. Introduction

[2] Various observational studies have found seasonal variations in the high-latitude ionospheric convection pattern and the cross-polar cap potential [*de la Beaujardière et al.*, 1991; *Weimer*, 1995; *Ruohoniemi and Greenwald*, 2005; *Zhang et al.*, 2007; *Pettigrew et al.*, 2010]. In general, the ionospheric convection is stronger and the cross-polar cap potential is larger near the equinoxes than near either of the solstices. This is similar to the well-known semiannual variation observed in geomagnetic activity, which also shows peaks near the equinoxes and troughs near the solstices [e.g., *Chapman and Bartels*, 1940; *McIntosh*, 1959; *Russell and McPherron*, 1973].

[3] Several studies [e.g., *Weimer*, 1995; *Pettigrew et al.*, 2010], rather than binning their data according to the actual season, binned their data according to the angle μ between the Earth's geomagnetic dipole axis and the geocentric solar magnetospheric (GSM) z axis, sometimes referred to as the "dipole tilt." We remind the reader that the GSM y axis is defined as perpendicular to the dipole axis, so that the dipole axis is always contained in the x-z plane. The x axis points from the Earth to the Sun, which means that the angle μ between the dipole axis and the z axis varies both as a function of season and as a function of time of day, due to the angle between the Earth's equatorial plane and the ecliptic plane ($\sim$23.5°) and the angle between the Earth's rotation axis and the dipole axis ($\sim$10°), respectively. We define μ as positive when the northern hemisphere (NH) is tilted toward the Sun. This means that on average, $\mu > 0$ at June solstice, $\mu < 0$ at December solstice, and $\mu = 0$ at the equinoxes, while superposed on this there is a daily variation consisting of a minimum in μ around 04:48 UT and a maximum around 16:48 UT, given the present-day longitude

[1]High Altitude Observatory, National Center for Atmospheric Research, Boulder, Colorado, USA.
[2]Thayer School of Engineering, Dartmouth College, Hanover, New Hampshire, USA.

Corresponding author: I. Cnossen, High Altitude Observatory, National Center for Atmospheric Research, 3080 Center Green Dr., Boulder, CO 80301, USA. (icnossen@ucar.edu)

0148-0227/12/2012JA017825

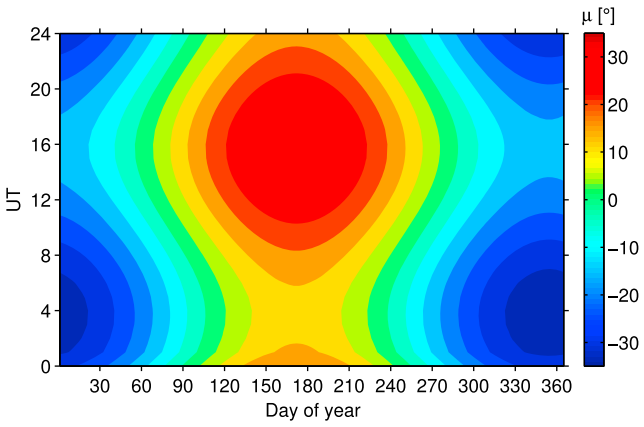

Figure 1. Diurnal and seasonal variation of the angle μ between the geomagnetic dipole axis and the GSM z axis.

(~72°W) of the NH geomagnetic pole. The diurnal and seasonal variation of μ is illustrated in Figure 1.

[4] *Pettigrew et al.* [2010] specifically showed that "seasonal" differences in high-latitude ionospheric convection are associated with μ rather than pure season. Variations in μ have also been put forward as one of the explanations for the semiannual variation in geomagnetic activity [e.g., *Svalgaard*, 1977; *Cliver et al.*, 2000, 2002; *Svalgaard et al.*, 2002]. Two main mechanisms by which μ may affect the magnetosphere-ionosphere system, and thereby the high-latitude ionospheric convection and geomagnetic activity, have been identified in the literature.

[5] First, a change in μ causes a change in the geometry between the Earth's magnetosphere and the solar wind, which may affect the solar wind–magnetosphere coupling. This is usually thought of as a modulation on the efficiency of the magnetic reconnection process, for which the orientation of the Earth's magnetic field with respect to the interplanetary magnetic field (IMF) is known to be important. It has been proposed that a modulation of the magnetic reconnection rate could take place within the magnetopause [*Crooker and Siscoe*, 1986] or in the length of the reconnection line [*Russell et al.*, 2003; *Nowada et al.*, 2009]. Both of these hypotheses predict a maximum reconnection rate when $\mu = 0°$, which could explain the observed maxima in cross-polar cap potential and geomagnetic activity near the equinoxes.

[6] A second possibility is that variations in ionospheric conductivity over the polar caps as the dipole axis tilts toward and away from the Sun affect the coupling between the ionosphere and the magnetosphere. Various mechanisms have been proposed to explain the semiannual variation in geomagnetic activity in this way [*Lyatsky et al.*, 2001; *Newell et al.*, 2002; *Nagatsuma*, 2006]. It is not immediately clear how it can explain the observed variations in cross-polar cap potential and high-latitude convection. In general, the cross-polar cap potential is expected to be smaller when the ionospheric conductivity is larger. This can be seen from equation (1), which follows from Ohm's law and current continuity:

$$\nabla_\perp \cdot (\Sigma \cdot \nabla_\perp \Phi) = J_\parallel \qquad (1)$$

where Φ is the electric field potential, Σ is the ionospheric conductance (the height-integrated conductivity), and $J_\parallel$ is the upward field-aligned current. If the upward field-aligned current stays constant, an increase in ionospheric conductance leads to a decrease in the electric field, which is usually associated with a reduction in the cross-polar cap potential. The ionospheric conductivity is on average largest in summer, intermediate at equinox, and smallest in winter, so that purely based on variations in ionospheric conductivity, one would expect the cross-polar cap potential to be largest in winter, followed by the equinoxes, and eventually summer, which is not what is observed. However, changes in the field-aligned currents could modify the expectations outlined above [e.g., *Ridley*, 2007; *Wiltberger et al.*, 2009], and ionospheric conductivity variations associated with μ could still affect the cross-polar cap potential in some way.

[7] In this study we aim to get a better understanding of the relative importance of variations in ionospheric conductivity and variations in solar wind–magnetosphere coupling associated with variations in μ. To do this, we make use of numerical model simulations in which we either keep the ionospheric conductance fixed or let it vary realistically with season and time of day. We also investigate in some detail how the variations in solar wind–magnetosphere coupling arise.

[8] This paper is organized as follows. In section 2 we describe the models that are used and the setup for the simulations in this study. The results are presented in section 3, which is divided into sections 3.1 and 3.2. In section 3.1 we discuss the main characteristics of the (semi)diurnal and seasonal variations associated with μ and compare the results for simulations with fixed and varying ionospheric conductance. In section 3.2 we investigate which processes contribute to the variations in solar wind–magnetosphere coupling identified in section 3.1. This is followed by a discussion in section 4 and our main conclusions in section 5.

2. Methods

[9] This study uses both simulations with the Lyon-Fedder-Mobarry (LFM) MHD code [*Lyon et al.*, 2004] and the Coupled Magnetosphere–Ionosphere-Thermosphere (CMIT) model [*Wiltberger et al.*, 2004; *Wang et al.*, 2004, 2008]. The latter is a combination of the LFM and the Thermosphere-Ionosphere-Electrodynamics general circulation model (TIE-GCM) [*Roble et al.*, 1988; *Richmond et al.*, 1992]. Both models have been described in detail in the references given above, so we only briefly discuss aspects here that are directly relevant to this study.

[10] The LFM solves the ideal MHD equations to simulate the interaction between the solar wind and the magnetosphere. While the LFM can accommodate a varying ionospheric conductance, in this study we set the conductance to a spatially and temporally constant value. This way, the influence that the ionospheric conductance might normally have on the coupling between the ionosphere and magnetosphere, and on the cross-polar cap potential, is switched off. For our purposes we set the Pedersen conductance to 5 S, while the Hall conductance was set to zero.

[11] In CMIT, the ionospheric conductivity is calculated from first principles within the thermosphere-ionosphere

part of the model, and varies realistically with solar illumination. This realistically varying conductance is used as a boundary condition for the magnetospheric part of the model. The magnetospheric part of the code in turn calculates the high-latitude electric potential and energetic particle precipitation fluxes and energies, which are fed back to the thermosphere-ionosphere part of the model. CMIT can thereby simulate the coupling between the magnetosphere and the ionosphere-thermosphere system, and variations in ionospheric conductance are able to influence this entire coupled system.

[12] Because CMIT and the LFM cannot realistically be run for an entire year to investigate seasonal variations in that way, we performed shorter (36 h) simulations at March equinox and June solstice. By comparing averages for equinox and solstice for both hemispheres we can gain some direct information on seasonal variations in cross-polar cap potential and field-aligned currents, and their relationship to variations in ionospheric conductance. We also study the (semi)diurnal variations in these variables that are produced by variations in μ. Both give us insight in the same mechanisms by which variations in μ affect the magnetosphere-ionosphere system and its coupling with the solar wind.

[13] The simulations with both models were set up in the same way as described by *Cnossen et al.* [2011]. The Earth's magnetic field was approximated by a centered dipole, with the NH geomagnetic pole at 80°N, 70°W. Each simulation started at 00:00 UT on 21 March (equinox) or 21 June (solstice), and was run for 36 h. We used a moderate solar activity level (F10.7 = 150) and idealized solar wind conditions. The solar wind density was set to a constant value of 5 cm^{-3}, and the outward solar wind speed was set to 400 km/s, while the speed in the GSM y and z directions was set to zero. The sound speed of the plasma in the solar wind was set to a constant 40 km/s, ensuring that the incoming solar wind was highly supersonic. We focus our analysis on simulations for which the GSM B_z component of the IMF was set to −5 nT for the first 2 h (00:00–02:00 UT), +5 nT for the second 2 h (02:00–04:00 UT), and −5 nT for the rest of the simulation, while the GSM B_x and B_y components were set to zero for the full duration of the simulations. We also performed a set of simulations in which the IMF B_z component remained northward after 04:00 UT and an additional set in which the IMF was set to zero throughout. Only the last 24 h of the simulations were used for analysis to allow a quasi-steady state to be reached.

3. Results

3.1. Daily and Seasonal Variations: CMIT Versus LFM

[14] Figure 2 shows the diurnal variation of a number of variables for both equinox and solstice and for both the CMIT and LFM simulations under southward IMF conditions. The first panel shows the angle μ, which is of course the same for CMIT and the LFM. The second to seventh panels show the NH and SH cross-polar cap potential, the NH and SH Pedersen conductance, and the NH and SH field-aligned currents. The Pedersen conductance is an average over magnetic latitudes >45°, and the field-aligned currents are the absolute value of the currents integrated over the same area. The eighth panel is discussed in section 3.2. The 24 h means and standard deviations of the variables mentioned above are shown in Figure 3 (organized by season) and are also given in Table 1.

[15] Let us first consider the CMIT results (solid lines in Figure 2), starting with the cross-polar cap potential. The cross-polar cap potentials for both hemispheres clearly show periodic variations, which are in phase with each other. Maxima in the cross-polar cap potentials are associated with minima in the absolute value of μ, which we will refer to as μ_{abs}, and vice versa. During equinox, μ_{abs} passes through a maximum and minimum twice per day, resulting in a semidiurnal (12 h period) variation in the cross-polar cap potentials, while μ_{abs} passes only once per day through a maximum and minimum during solstice, resulting in a diurnal (24 h period) variation. The average value of μ_{abs} is higher during solstice than during equinox, and correspondingly, the average cross-polar cap potential is lower during solstice than during equinox, by ∼42 kV on average (see Table 1 and Figure 3).

[16] It matters slightly whether μ is positive or negative, or in other words, whether a given hemisphere is tilted toward or away from the Sun. When the hemisphere in question is tilted toward the Sun, the minimum in the cross-polar cap potential is deeper than when that hemisphere is tilted away from the Sun. For instance, the NH solstice (summer) minimum is ∼10 kV deeper than the SH solstice (winter) minimum, and there is a similar difference between the first and second minima at equinox within the same hemisphere. The average cross-polar cap potential at solstice in the summer hemisphere (NH) is also ∼10 kV lower than in the winter hemisphere (SH).

[17] We can explain the differences between the summer and winter hemispheres, and the differences between the two daily minima in the same hemisphere at equinox, through the difference in ionospheric conductance. When the hemisphere in question is tilted toward the Sun (in summer or at 16.40 (04:40) UT for the NH (SH) at equinox), the ionospheric conductance is higher than when it is tilted away from the Sun. From equation (1) it follows that a higher conductance leads to a lower electric potential gradient (i.e., electric field), and/or stronger field-aligned currents. A weaker electric field is usually associated with a smaller cross-polar cap potential, unless the distance between the potential maximum and minimum changes. Whenever a given hemisphere is tilted toward the Sun, this therefore tends to lead to a relatively smaller cross-polar cap potential. The LFM results confirm this reasoning. There are still (semi)diurnal variations in the cross-polar cap potentials, similar to the ones found for CMIT, and there is still a ∼35 kV difference between equinox and solstice, but there is no noticeable difference between the summer and winter hemispheres or between the two minima in the same hemisphere at equinox.

[18] We now turn our attention to the daily variations in the field-aligned currents, again considering the CMIT results first. At equinox, the field-aligned currents show a diurnal (24 h period) variation that is in phase with the variation in the conductance. There is a 12 h phase shift between the two hemispheres, as maxima and minima occur in each hemisphere when that hemisphere is tilted toward and away from the Sun, respectively. At solstice, a similar diurnal variation in the field-aligned currents exists in the SH, but not in the NH. In that hemisphere, the diurnal variation in the cross-polar cap potential is 12 h out of phase with the diurnal variation in the conductance, and the effects of both variations

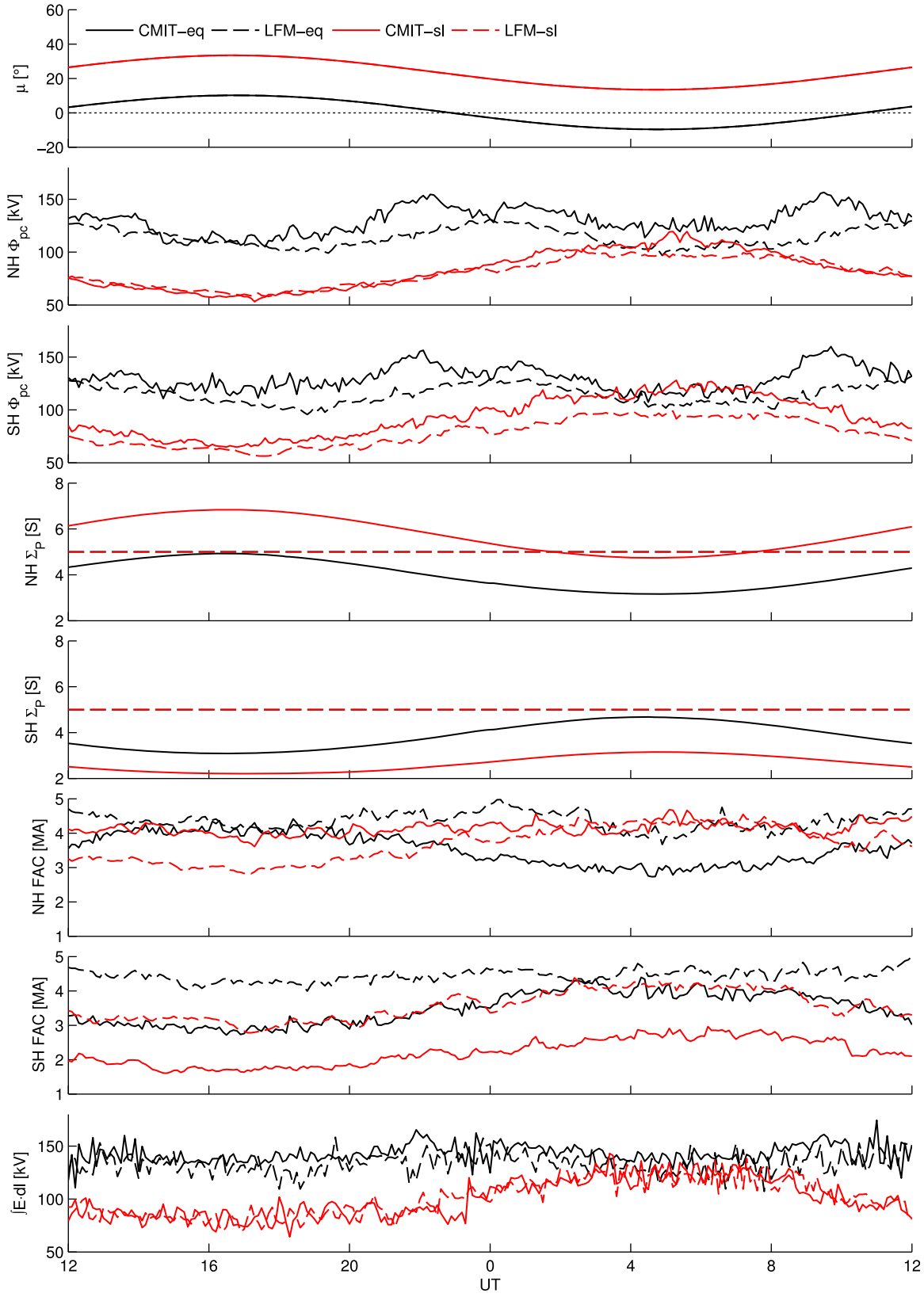

Figure 2. From top to bottom, the angle μ between the geomagnetic dipole axis and the GSM z axis, the NH and SH cross-polar cap potential Φ_{pc}, the NH and SH Pedersen conductance Σ_P averaged over magnetic latitudes >45°, the NH and SH total vertical field-aligned current (FAC) integrated over magnetic latitudes >45°, and the integral of the electric field parallel to the dayside separator line $\int \mathbf{E} \cdot \mathbf{dl}$ as a function of UT for the CMIT and LFM March equinox and June solstice simulations for southward IMF.

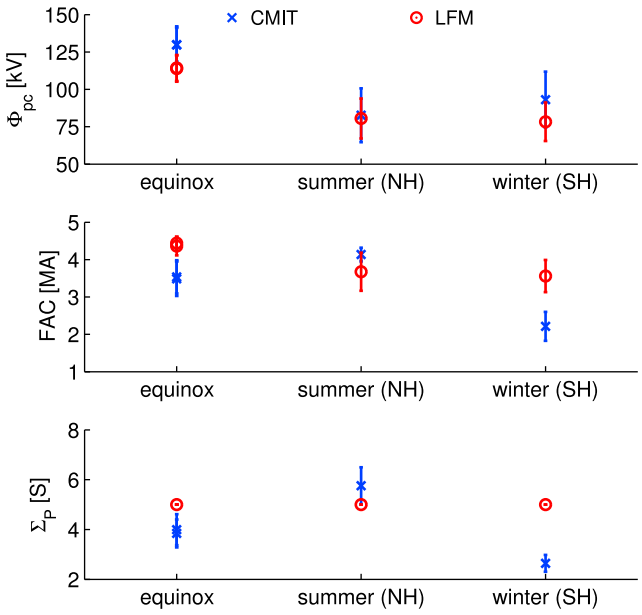

Figure 3. The 24 h mean values of the cross-polar cap potential Φ_{pc}, the Pedersen conductance Σ_P averaged over magnetic latitudes >45°, and the total vertical field-aligned current (FAC) integrated over magnetic latitudes >45°, organized by season, for the CMIT and LFM simulations for southward IMF. The error bars represent the standard deviations.

appear to balance each other in this case, so that little variation in the field-aligned currents is seen.

[19] The 24 h mean of the field-aligned currents is largest in summer, followed by equinox, and eventually winter (see Table 1 and Figure 3). This more or less follows the seasonal variation seen in the ionospheric conductance, although the difference between equinox and summer is not as pronounced in the field-aligned currents as in the ionospheric conductance. This is related to the larger cross-polar cap potential at equinox, which also influences the field-aligned currents. Still, the variations in the field-aligned currents seem to be mostly controlled by variations in ionospheric conductance. This is again confirmed by the LFM simulations, which show much smaller seasonal differences in the field-aligned currents than found with CMIT, and no difference at all between the summer and winter hemispheres.

[20] The LFM simulations do still show differences between the 24 h solstice and equinox means of the cross-polar cap potential and field-aligned currents, as well as (semi)diurnal variations. The LFM cross-polar cap potentials vary with UT in a similar way as the CMIT cross-polar cap potentials, but the amplitudes are somewhat reduced. To quantify this we fitted a sinusoidal function of the following form to the cross-polar cap potential time series:

$$f(t) = a + b \cdot \sin(2\pi t + \alpha) \quad (2)$$

The amplitudes b are given in Table 2. These numbers show that at solstice the LFM amplitudes are ~70% of the CMIT amplitudes, while at equinox this is ~85–90%. We can therefore conclude that variations in solar wind–magnetosphere coupling are responsible for 70–90% of the (semi)diurnal variation in the cross-polar cap potential, while variations in ionospheric conductance are responsible for the remainder. We also note that there appears to be a phase shift between the LFM and CMIT, in particular at equinox, when all maxima and minima in the cross-polar cap potential occur ~1.5 h later for the LFM. At solstice there is a much smaller phase shift, if any.

[21] At solstice, the diurnal variation in the LFM field-aligned currents is in phase with the variation in the cross-polar cap potential, which is expected from equation (1), given the fixed ionospheric conductance. However, during equinox, the field-aligned currents do not show much variation. This means that the variation that is seen in the cross-polar cap potential during equinox must be balanced by changes in the distance between the potential maxima and minima, in order for equation (1) to remain satisfied. We indeed find a semidiurnal variation in this distance that is more or less in phase with the semidiurnal variation in the cross-polar cap potential (not shown). We also find a diurnal variation in the distance between the maximum and minimum potential during solstice (not shown), but apparently this is not sufficient then to cancel out the variation in the cross-polar cap potential itself. The daily variations in the field-aligned currents for the LFM are quite different from those calculated with CMIT, so that it does not make much sense to compare their amplitudes, as was done for the cross-polar cap potential, and quantify the influence of the ionospheric conductance that way. However, the fact that the variations are so different is evidence in itself that the ionospheric conductance plays an important role in causing/modifying them.

[22] So far we have only discussed results for southward IMF. Under northward IMF conditions the cross-polar cap potentials and field-aligned currents become much smaller,

Table 1. Means and Standard Deviations (σ) Over the Last 24 h of the CMIT and LFM Simulations for the NH and SH Cross-Polar Cap Potential, Pedersen Conductance and Field-Aligned Currents for Equinox and Solstice for Southward IMF

		Φ_{pc} (kV)				Σ_P (S)				FAC (MA)			
		NH		SH		NH		SH		NH		SH	
	Simulation	Mean	σ	Mean	σ	Mean	σ	Mean	σ	Mean	σ	Mean	σ
Equinox	CMIT	129.7	12.4	129.9	11.2	4.0	0.6	3.8	0.6	3.5	0.4	3.5	0.5
	LFM	113.9	8.8	114.3	8.7	5.0	0.0	5.0	0.0	4.4	0.2	4.4	0.2
Solstice	CMIT	82.7	18.0	93.1	18.7	5.8	0.7	2.6	0.3	4.1	0.2	2.2	0.4
	LFM	80.4	13.4	78.3	12.9	5.0	0.0	5.0	0.0	3.7	0.5	3.6	0.4

Table 2. Amplitude of the (Semi)Diurnal Variation in the Cross-Polar Cap Potential (kV) at Equinox and Solstice for CMIT and the LFM Under Southward IMF as Determined From Fits of the Time Series to Equation (2)

	Equinox		Solstice	
	NH	SH	NH	SH
CMIT	13.9	12.6	25.4	26.0
LFM	11.7	11.5	18.5	17.9

as expected. We can still identify (semi)diurnal and seasonal variations that appear similar in character to those found under southward IMF, but they are also much smaller, and therefore relatively more affected by random variability. For example, the amplitude of the variation in cross-polar cap potential under northward IMF, obtained by fits to equation (2), is on the order of 1–2 kV for CMIT and <1 kV for the LFM, while standard deviations are on the order of 0.5–1 kV. It thus becomes questionable that any meaningful results can be obtained from a more detailed analysis, and we will therefore restrict ourselves to southward IMF conditions only from now on.

3.2. Effect of μ on Solar Wind–Magnetosphere Coupling

[23] The differences between solstice and equinox, as well as the (semi)diurnal variations found in the LFM simulations can only be explained through the effects of variations in μ on the coupling between the magnetosphere and the solar wind, because there is no other source for such systematic variations. We now investigate the processes responsible for the variation in solar wind–magnetosphere coupling in some more detail.

[24] As a first test to check whether these variations are associated with a modulation of the magnetic reconnection process, we performed an additional LFM simulation for equinox with zero IMF, so that magnetic reconnection cannot occur. We do still find a weak periodic variation in the cross-polar cap potentials in this case (not shown), consisting mainly of small (~7–8 kV) increases around 12:00 and 24:00 UT on top of a more or less constant base value of ~20–22 kV. These increases must be related to changes in the viscous interaction between the solar wind and the magnetosphere [see, e.g., *Lopez et al.*, 2012]. The peaks in viscous interaction at 12:00 and 24:00 UT are probably due to the magnetosphere forming a stronger obstacle that the solar wind must flow around when $\mu = 0$ (at 10:42 and 22:42 UT). The 1–1.5 h delay in the occurrence of the peaks in the cross-polar cap potential is similar to that seen in the original LFM simulations and may in part reflect the time needed for the effect to be communicated from the magnetosphere to the ionosphere, although 1–1.5 h seems too long to be just a communication time lag. Nevertheless, the variation in the cross-polar cap potential produced this way is small, and by no means sufficient to explain the (semi) diurnal variation seen in the original LFM simulations. From this we can conclude that the magnetic reconnection process must contribute to the variations associated with μ.

[25] We investigate this further by examining the characteristics of the dayside magnetic reconnection in our simulations. Previous work [e.g., *Siscoe et al.*, 2001; *Dorelli et al.*, 2007] has shown that the rate and distribution of magnetopause reconnection can be characterized by the component of the electric field along the line where the solar wind and Earth magnetic field lines merge, the separator line. Regions with a strong electric field parallel to this line are regions of high reconnection activity. The rate of dayside reconnection is given by $\varphi_{day} = \int \mathbf{E} \cdot \mathbf{dl}$, where the integral is done over the dayside separator line. We determined the location of the separator line by tracing field lines from points lying in a plane of constant local time and determining whether the field lines were of open, closed, or solar wind topology. Open field lines have one foot point either connected to the NH or the SH, so that there are four topology classes in total. The separator line at each longitude was defined as the point where all four topologies merged in the plane that the field lines were traced from [see also *Laitinen et al.*, 2006]. The search was carried out over the region of the magnetopause where $X > 0$, i.e., over the region of 06:00 to 18:00 LT.

[26] The potential drop across the separator line, i.e., $\int \mathbf{E} \cdot \mathbf{dl}$, maps down to the polar caps in the ionosphere via magnetic field lines, and should equal the cross-polar cap potential in case of perfectly time-steady conditions and zero field-aligned potential drops [*Ouellette et al.*, 2010]. In our simulations these conditions are only approximately satisfied. Departures from a steady state occur, and small nonzero field-aligned potential drops can arise from numerical errors of the solutions to the ideal MHD equations. We do explicitly set the field-aligned potential drop between the inner magnetosphere boundary and the ionosphere to zero. In addition, the foot points of the field lines at the maximum and minimum points of the polar cap potential field may not map exactly to the points on the separator line where we defined our bounds of integration to calculate $\int \mathbf{E} \cdot \mathbf{dl}$. For these reasons $\int \mathbf{E} \cdot \mathbf{dl}$ and the cross-polar cap potential are unlikely to be in exact agreement, but they should be comparable.

[27] Figure 2 shows $\int \mathbf{E} \cdot \mathbf{dl}$ as a function of UT for each of our simulations. There are indeed some differences between $\int \mathbf{E} \cdot \mathbf{dl}$ and the cross-polar cap potentials: $\int \mathbf{E} \cdot \mathbf{dl}$ displays considerably more short-term variability and is generally ~20 kV higher. However, $\int \mathbf{E} \cdot \mathbf{dl}$ does show a (semi)diurnal variation similar to the variation in the cross-polar cap potential, as well as a similar difference between equinox and solstice. This confirms that changes in the reconnection rate are an important contributor to the variation associated with μ in the cross-polar cap potential.

[28] There is also a 0.5–1 h phase shift in $\int \mathbf{E} \cdot \mathbf{dl}$ between the CMIT and LFM simulations at equinox, which could explain the phase shift between CMIT and the LFM seen in the cross-polar cap potential at least partly. In addition, CMIT appears to show on average a higher $\int \mathbf{E} \cdot \mathbf{dl}$ than the LFM at equinox, while there is no such difference at solstice. It is not clear whether these differences between CMIT and LFM at equinox are "real," in which case they would imply an influence of the ionospheric conductance on the reconnection process, or whether they are simply due to inaccuracies, i.e., noise. We leave this as a topic for future studies.

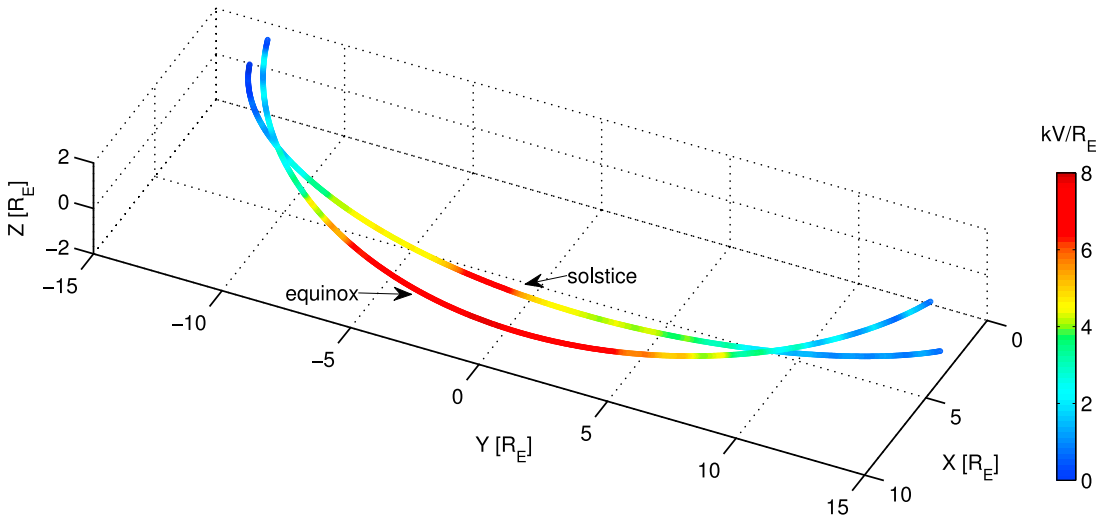

Figure 4. The 24 h mean position of the separator line for March equinox and June solstice for the CMIT simulations for southward IMF, color-coded with the mean strength of the electric field parallel to the separator line.

[29] To determine where the differences in $\int \mathbf{E} \cdot \mathbf{dl}$ come from, we compare the CMIT equinox and solstice results in Figure 4. This shows the 24 h mean positions of the separator line for both seasons, color-coded with the mean strength of the parallel electric field along the line. At equinox, there is a broad region of relatively high parallel electric field, while this is clearly much narrower at solstice. A relatively high rate of magnetic reconnection thus occurs over a much wider extent for equinox than for solstice. Diurnal variations in reconnection rate are probably due to similar variations in the length over which reconnection occurs, but this is more difficult to show due to the strong short-term variability.

[30] The distribution of magnetic reconnection at equinox and solstice is further studied in Figure 5, which shows the electric field parallel to the separator line versus distance along this line, moving from dawn to dusk, for both CMIT and the LFM. Again, it is clear that relatively strong reconnection takes place along a much narrower section of the separator line for solstice than for equinox. There is also a difference between the LFM and CMIT at equinox, which corresponds to the higher $\int \mathbf{E} \cdot \mathbf{dl}$ for CMIT seen Figure 2 discussed earlier. To quantify the differences in the length over which strong reconnection takes place, we may take a certain threshold of the parallel electric field and calculate the length of the section of the separator line with a parallel electric field greater than that threshold. Using a threshold of 5 kV/R_E, this comes to 14.5 R_E for equinox compared to 3.5 R_E for solstice when using the CMIT results, or to 13.6 R_E for equinox and 3.4 R_E for solstice for the LFM.

4. Discussion

[31] Our results for southward IMF show that the cross-polar cap potential is larger at equinox than at solstice, in qualitative agreement with observations. The CMIT simulations show a difference of ∼42 kV between equinox and solstice, while this is ∼35 kV for the LFM simulations. While this difference amounts to ∼30% of the equinox value in both cases, the LFM equinox/solstice difference is ∼17% smaller than the CMIT difference, which may be interpreted as the influence of the ionospheric conductance. The remainder of the equinox/solstice differences (∼83%) must then be attributed to differences in solar wind–magnetosphere coupling. The (semi)diurnal variations in the cross-polar cap potential for the LFM and CMIT suggest that the ionospheric conductance is responsible for 10–15% (equinox) or ∼30% (solstice) of those variations. Variations in the cross-polar cap potential thus seem to be largely (70–90%) due to variations in solar wind–magnetosphere coupling. A recent study by *Palmroth et al.* [2012] also demonstrated that there is a seasonal difference in this coupling. Their

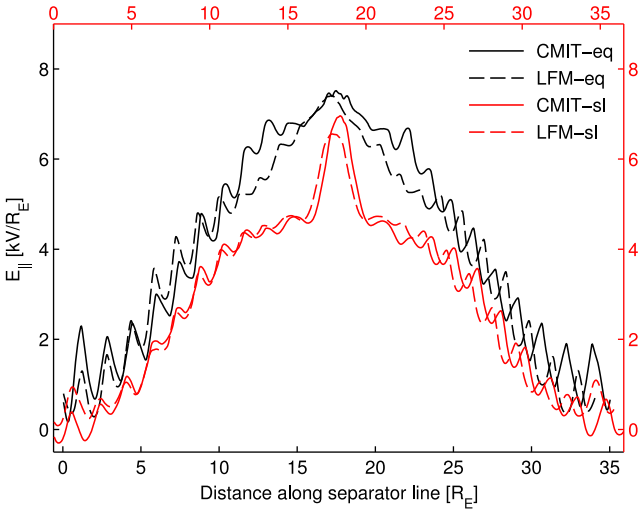

Figure 5. The 24 h mean strength of the electric field parallel to the separator line as a function of distance along the separator line from dawn to dusk for the CMIT and LFM March equinox and June solstice simulations for southward IMF.

simulations showed a ~10% larger energy transfer from the solar wind to the magnetosphere at equinox compared to solstice. While this difference is smaller than what we report here, it agrees qualitatively with our results. *Palmroth et al.* [2012] also noted that the energy transfer at solstice takes place preferably in the summer hemisphere. This is again consistent with our results, as we find that the separator line is tilted within the GSM *x-z* plane, such that the subsolar point on the separator line is in the summer hemisphere, and its tailward end in the winter hemisphere, although this is difficult to see in Figure 4.

[32] Most of the variation in solar wind–magnetosphere coupling is due to the dependence of the magnetic reconnection rate on μ, estimated as $\int \mathbf{E} \cdot \mathbf{dl}$, the integral of the electric field parallel to the separator line. Comparing the distribution of the electric field parallel to the separator line between solstice and equinox, we found that the difference in $\int \mathbf{E} \cdot \mathbf{dl}$ is mainly due to a wider region over which relatively strong reconnection takes place at equinox compared to solstice. This agrees at least qualitatively with *Russell et al.* [2003], who used simulations with northward IMF, and estimated the neutral line length based on the locations where the IMF was parallel to the Earth's magnetic field, assuming that this would be where magnetic reconnection would have occurred if the IMF had been southward. They showed that for due "southward" IMF the reconnection line extends over a ~170° longitudinal width for $\mu = 0$, while this drops to ~27° for $\mu = 15°$ and ~6° for $\mu = 30°$.

[33] Considering that magnetic reconnection plays a key role in causing the variations in the cross-polar cap potential with μ, it may be expected that these variations will depend on the orientation of the IMF. In this study we focused on due southward IMF conditions. However, observational studies have noted that the dependence of the ionospheric convection patterns on μ depends on the direction of the IMF, and *Russell et al.* [2003] found that the reconnection line length depends less strongly on μ for IMF orientations away from due south (down to a clock angle of 135°). Our simulations for northward IMF also indicated much weaker (semi)diurnal and seasonal variations in cross-polar cap potential. We must therefore bear in mind that in the real world, where the IMF constantly changes direction, the variation in cross-polar cap potential with μ is likely to be less pronounced than simulated here. Additionally, variations in solar wind speed and density may introduce variability in the cross-polar cap potential, further obscuring variations associated with μ.

[34] While solstice/equinox differences are mostly associated with differences in solar wind–magnetosphere coupling, according to our results, any differences between summer and winter must be entirely due to differences in ionospheric conductance, as we find no difference between the NH and SH during solstice for the LFM simulations. For CMIT the cross-polar cap potential is slightly higher in winter than in summer, though this difference may not be significant. Observational studies are not conclusive either, with some studies reporting a larger cross-polar cap potential in winter [*de la Beaujardière et al.*, 1991; *Zhang et al.* 2007], and others a larger cross-polar cap potential in summer [*Weimer*, 1995; *Ruohoniemi and Greenwald*, 2005; *Pettigrew et al.*, 2010]. Further work is thus needed to establish convincingly whether a summer/winter difference exists, and if so, in what sense.

[35] The variation in cross-polar cap potential associated with the variations in μ is likely to have consequences for the rest of the thermosphere-ionosphere system. For instance, changes in high-latitude ionospheric convection and conductance will lead to changes in the neutral winds and changes in Joule heating, which will in turn affect the thermospheric temperature structure. These effects are further explored by *Cnossen and Richmond* [2012] using simulations with different dipole axis tilts. Here we just comment briefly on the implications for geomagnetic activity.

[36] Geomagnetic activity arises from the perturbations to the Earth's magnetic field caused by currents flowing in the ionosphere and magnetosphere. As mentioned in the introduction, there is a semiannual variation in geomagnetic activity that can be explained by up to 65% through variations in μ [*Cliver et al.*, 2000]. Changes in solar wind–magnetosphere coupling are expected to affect geomagnetic activity, and since we have shown that this coupling does vary with μ, it is likely that this controls part of the semiannual variation in geomagnetic activity. On the other hand, *Svalgaard* [2011] showed that this semiannual variation is still present under northward IMF conditions, albeit somewhat weaker than under southward IMF, while we find only very weak variations in cross-polar cap potentials under northward IMF, indicative of only weak variations in solar wind–magnetosphere coupling. This suggests that variations in ionospheric conductance play a more important role in this case. Indeed, we showed that the ionospheric conductance plays a relatively more important role in variations in the field-aligned currents than in variations in the cross-polar cap potentials, and it is well known that other current systems in the ionosphere also depend strongly on ionospheric conductivity. The portion of the semiannual variation in geomagnetic activity that is associated with variations in μ may therefore be related more closely to variations in ionospheric conductance than variations in solar wind–magnetosphere coupling. Alternatively, there could be other ways in which solar wind–magnetosphere coupling affects geomagnetic activity, not necessarily involving the magnetic reconnection process. For instance, *Azpilicueta and Brunini* [2012] recently argued, following an earlier suggestion by *Malin and Isikara* [1976], that variations in μ result in deformations of the shape of the magnetospheric cavity in which the ring current flows and that these could contribute to (semi)annual variations in magnetic perturbations on the ground. We were not able to test this hypothesis here, however, since CMIT does not yet give an accurate representation of the ring current.

5. Conclusions

[37] We investigated how daily and seasonal variations in the angle μ between the geomagnetic dipole axis and the GSM *z* axis influence the cross-polar cap potential. We specifically examined the role of variations in solar wind–magnetosphere coupling and the role of variations in the ionospheric conductance over the polar caps under

southward IMF conditions. We find that variations in ionospheric conductance contribute to the variations in the cross-polar cap potential with μ, but they play a relatively minor role in explaining the differences between equinox and solstice. Most of these differences (70–90%) are due to changes in solar wind–magnetosphere coupling. A small portion of this may be associated with viscous processes, but the dominant contributor is the variation in the magnetic reconnection rate with μ. The magnetic reconnection rate, here estimated as the integral of the electric field parallel to the separator line, $\int \mathbf{E} \cdot \mathbf{dl}$, maximizes when $\mu = 0$, and progressively decreases when μ moves further away from zero (in either direction). By comparing the 24 h mean distribution of the parallel electric field along the separator line for equinox and solstice, we showed that relatively strong reconnection, indicated by a relatively strong parallel electric field, occurs over a much longer section of the reconnection line at equinox than at solstice. Differences in this line length seem to be primarily responsible for the difference in cross-polar cap potential between solstice and equinox, and are likely to be responsible for most of the (semi)diurnal variation as well. On the other hand, the variations in the field-aligned currents, while still in part controlled by variations in solar wind–magnetosphere coupling, are also strongly influenced by variations in ionospheric conductance. The same may be true for the semiannual variation in geomagnetic activity.

[38] **Acknowledgments.** Part of this work was supported by NASA grants NNH07AF041 and NNX08AG09G. The National Center for Atmospheric Research is sponsored by the National Science Foundation. We thank Gang Lu and two anonymous reviewers for thoughtful comments on earlier versions of this manuscript.

[39] Philippa Browning thanks the reviewers for their assistance in evaluating this paper.

References

Azpilicueta, F., and C. Brunini (2012), A different interpretation of the annual and semiannual anomalies on the magnetic activity over the Earth, *J. Geophys. Res.*, *117*, A08202, doi:10.1029/2012JA017893.

Chapman, S., and J. Bartels (1940), *Geomagnetism*, Clarendon, Oxford, U. K.

Cliver, E. W., Y. Kamide, and A. G. Ling (2000), Mountains versus valleys: Semiannual variation of geomagnetic activity, *J. Geophys. Res.*, *105*(A2), 2413–2424, doi:10.1029/1999JA900439.

Cliver, E. W., Y. Kamide, and A. G. Ling (2002), The semiannual variation of geomagnetic activity: Phases and profiles for 130 years of *aa* data, *J. Atmos. Sol. Terr. Phys.*, *64*, 47–53, doi:10.1016/S1364-6826(01)00093-1.

Cnossen, I., and A. D. Richmond (2012), How changes in the tilt angle of the geomagnetic dipole affect the coupled magnetosphere-ionosphere-thermosphere system, *J. Geophys. Res.*, *117*, A10317, doi:10.1029/2012JA018056.

Cnossen, I., A. D. Richmond, M. Wiltberger, W. Wang, and P. Schmitt (2011), The response of the coupled magnetosphere-ionosphere-thermosphere system to a 25% reduction in the dipole moment of the Earth's magnetic field, *J. Geophys. Res.*, *116*, A12304, doi:10.1029/2011JA017063.

Crooker, N. U., and G. L. Siscoe (1986), On the limits of energy transfer through dayside merging, *J. Geophys. Res.*, *91*(A12), 13,393–13,397, doi:10.1029/JA091iA12p13393.

de la Beaujardière, O., D. Alcayde, J. Fontanari, and C. Leger (1991), Seasonal dependence of high-latitude electric fields, *J. Geophys. Res.*, *96*(A4), 5723–5735, doi:10.1029/90JA01987.

Dorelli, J. C., A. Bhattacharjee, and J. Raeder (2007), Separator reconnection at Earth's dayside magnetopause under generic northward interplanetary magnetic field conditions, *J. Geophys. Res.*, *112*, A02202, doi:10.1029/2006JA011877.

Laitinen, T. V., P. Janhunen, T. I. Pulkkinen, M. Palmroth, and H. E. J. Koskinen (2006), On the characterization of magnetic reconnection in global MHD simulations, *Ann. Geophys.*, *24*, 3059–3069, doi:10.5194/angeo-24-3059-2006.

Lopez, R. E., S. K. Bhattarai, R. Bruntz, K. Pham, M. Wiltberger, J. G. Lyon, Y. Deng, and Y. Huang (2012), The role of dayside merging in generating the ionospheric potential during the Whole Heliosphere Interval, *J. Atmos. Sol. Terr. Phys.*, *83*, 63–69, doi:10.1016/j.jastp.2012.03.001.

Lyatsky, W., P. T. Newell, and A. Hamza (2001), Solar illumination as cause of the equinoctial preference for geomagnetic activity, *Geophys. Res. Lett.*, *28*(12), 2353–2356, doi:10.1029/2000GL012803.

Lyon, J. G., J. A. Fedder, and C. M. Mobarry (2004), The Lyon-Fedder-Mobarry (LFM) global MHD magnetospheric simulation code, *J. Atmos. Sol. Terr. Phys.*, *66*, 1333–1350, doi:10.1016/j.jastp.2004.03.020.

Malin, S. R., and A. M. Isikara (1976), Annual variation of the geomagnetic field, *Geophys. J. R. Astron. Soc.*, *47*, 445–457, doi:10.1111/j.1365-246X.1976.tb07096.x.

McIntosh, D. H. (1959), On the annual variation of magnetic disturbance, *Philos. Trans. R. Soc. London, Ser. A*, *251*, 525–552, doi:10.1098/rsta.1959.0010.

Nagatsuma, T. (2006), Diurnal, semiannual, and solar cycle variations of solar wind–magnetosphere-ionosphere coupling, *J. Geophys. Res.*, *111*, A09202, doi:10.1029/2005JA011122.

Newell, P. T., T. Sotirelis, J. P. Skura, and C.-I. Meng (2002), Ultraviolet insolation drives seasonal and diurnal space weather variations, *J. Geophys. Res.*, *107*(A10), 1305, doi:10.1029/2001JA000296.

Nowada, M., J.-H. Shue, and C. T. Russell (2009), Effects of dipole tilt angle on geomagnetic activity, *Planet. Space Sci.*, *57*, 1254–1259, doi:10.1016/j.pss.2009.04.007.

Ouellette, J. E., B. N. Rogers, M. Wiltberger, and J. G. Lyon (2010), Magnetic reconnection at the dayside magnetopause in global Lyon-Fedder-Mobarry simulations, *J. Geophys. Res.*, *115*, A08222, doi:10.1029/2009JA014886.

Palmroth, M., R. C. Fear, and I. Honkonen (2012), Magnetopause energy transfer dependence on the interplanetary magnetic field and the Earth's magnetic dipole axis orientation, *Ann. Geophys.*, *30*, 515–526, doi:10.5194/angeo-30-515-2012.

Pettigrew, E. D., S. G. Shepherd, and J. M. Ruohoniemi (2010), Climatological patterns of high-latitude convection in the Northern and Southern Hemispheres: Dipole tilt dependencies and interhemispheric comparisons, *J. Geophys. Res.*, *115*, A07305, doi:10.1029/2009JA014956.

Richmond, A. D., E. C. Ridley, and R. G. Roble (1992), A thermosphere/ionosphere general circulation model with coupled electrodynamics, *Geophys. Res. Lett.*, *19*(6), 601–604, doi:10.1029/92GL00401.

Ridley, A. J. (2007), Effects of seasonal changes in the ionospheric conductances on magnetospheric field-aligned currents, *Geophys. Res. Lett.*, *34*, L05101, doi:10.1029/2006GL028444.

Roble, R. G., E. C. Ridley, A. D. Richmond, and R. E. Dickinson (1988), A coupled thermosphere/ionosphere general circulation model, *Geophys. Res. Lett.*, *15*(12), 1325–1328, doi:10.1029/GL015i012p01325.

Ruohoniemi, J. M., and R. A. Greenwald (2005), Dependencies of high-latitude plasma convection: Consideration of interplanetary magnetic field, seasonal, and universal time factors in statistical patterns, *J. Geophys. Res.*, *110*, A09204, doi:10.1029/2004JA010815.

Russell, C. T., and R. L. McPherron (1973), Semi-annual variation of geomagnetic activity, *J. Geophys. Res.*, *78*(1), 92–108, doi:10.1029/JA078i001p00092.

Russell, C. T., Y. L. Wang, and J. Raeder (2003), Possible dipole tilt dependence of dayside magnetopause reconnection, *Geophys. Res. Lett.*, *30*(18), 1937, doi:10.1029/2003GL017725.

Siscoe, G. L., G. M. Erickson, B. U. Ö. Sonnerup, N. C. Maynard, K. D. Siebert, D. R. Weimer, and W. W. White (2001), Global role of $E_{||}$ in magnetopause reconnection: An explicit demonstration, *J. Geophys. Res.*, *106*(A7), 13,015–13,022, doi:10.1029/2000JA000062.

Svalgaard, L. (1977), Geomagnetic activity: Dependence on solar wind parameters, in *Coronal Holes and High Speed Wind Streams*, edited by J. B. Zirker, pp. 371–441, Colo. Assoc. Univ. Press, Boulder.

Svalgaard, L. (2011), Geomagnetic semiannual variation is not overestimated and is not an artefact of systematic solar hemispheric asymmetry, *Geophys. Res. Lett.*, *38*, L16107, doi:10.1029/2011GL048616.

Svalgaard, L., E. W. Cliver, and A. G. Ling (2002), The semiannual variation of great geomagnetic storms, *Geophys. Res. Lett.*, *29*(16), 1765, doi:10.1029/2001GL014145.

Wang, W., M. Wiltberger, A. G. Burns, S. C. Solomon, T. L. Killeen, N. Maruyama, and J. G. Lyon (2004), Initial results from the coupled magnetosphere-ionosphere-thermosphere model: Thermosphere-ionosphere responses, *J. Atmos. Sol. Terr. Phys.*, *66*, 1425–1441, doi:10.1016/j.jastp.2004.04.008.

Wang, W. B., J. H. Lei, A. G. Burns, M. Wiltberger, A. D. Richmond, S. C. Solomon, T. L. Killeen, E. R. Talaat, and D. N. Anderson (2008), Ionospheric electric field variations during a geomagnetic storm simulated by a coupled magnetosphere ionosphere thermosphere (CMIT) model, *Geophys. Res. Lett.*, *35*, L18105, doi:10.1029/2008GL035155.

Weimer, D. R. (1995), Models of high-latitude electric potentials derived with a least error fit of spherical harmonic coefficients, *J. Geophys. Res.*, *100*(A10), 19,595–19,607, doi:10.1029/95JA01755.

Wiltberger, M., W. Wang, A. G. Burns, S. C. Solomon, J. G. Lyon, and C. C. Goodrich (2004), Initial results from the coupled magnetosphere ionosphere thermosphere model: Magnetospheric and ionospheric responses, *J. Atmos. Sol. Terr. Phys.*, *66*, 1411–1423, doi:10.1016/j.jastp.2004.03.026.

Wiltberger, M., R. S. Weigel, W. Lotko, and J. A. Fedder (2009), Modeling seasonal variations of auroral particle precipitation in a global-scale magnetosphere-ionosphere simulation, *J. Geophys. Res.*, *114*, A01204, doi:10.1029/2008JA013108.

Zhang, S.-R., J. M. Holt, and M. McCready (2007), High latitude convection based on long-term incoherent scatter radar observations in North America, *J. Atmos. Sol. Terr. Phys.*, *69*, 1273–1291, doi:10.1016/j.jastp.2006.08.017.